

Elsevier Editorial System(tm) for Journal of  
Alloys and Compounds  
Manuscript Draft

Manuscript Number: JALCOM-D-17-08498R2

Title: Phase equilibria in the Fe-Ce-C system at 1100°C

Article Type: Review Article

Keywords: Phase diagram, ternary compound, isothermal section, Fe-Ce-C,  
rare earth metal, phase equilibria, lanthanides,

Corresponding Author: Miss Masuma Mardani,

Corresponding Author's Institution: MISIS

First Author: Masuma Mardani

Order of Authors: Masuma Mardani; Iuliia Fartushna; Alexandra khvan;  
Vladimir cheverikin; Dmitri Ivanov; alexander kondratiev; Alan Dinsdale

Abstract: Phase equilibria in the Fe-Ce-C system at 1100°C were studied using X-ray diffraction, SEM and electron probe microanalysis. An isothermal section at this temperature was constructed covering the whole concentration range. The stability of the ternary compound  $\square 1$  at 1100°C, identified previously, was confirmed and its composition determined as 23Fe-29Ce-48C according our data. It is also confirmed that the ternary compound  $\square 1$  does not have a homogeneity range. The liquid phase is stable at 1100°C in the Fe-Ce-C system. The isothermal section is characterized by five three-phase regions:  $(\gamma\text{Fe}) + (\text{C}) + (\alpha\text{CeC}_2)$ ,  $(\gamma\text{Fe}) + \square 1 + (\alpha\text{CeC}_2)$ ,  $(\gamma\text{Fe}) + \square 1 + (\text{Ce}_2\text{C}_3)$ ,  $(\alpha\text{CeC}_2) + \square 1 + (\text{Ce}_2\text{C}_3)$  and  $\text{L} + (\gamma\text{Fe}) + (\text{Ce}_2\text{C}_3)$  plus the corresponding two-phase regions.

Dear Editor,

We would like to submit our paper “**Phase equilibria in the Fe-C-Ce system at 1100°C**” for publication in the [Journal of alloys and compounds](#). We confirm that this paper represents the authors’ own work and that it has not been submitted to any other journal. We also confirm that all authors have read the manuscript and agreed to submit it. We hope that our manuscript will be accepted for the editorial processing. We are looking forward for your reply.

Best regards,

M. Mardani, I. Fartushna, A. Khvan, V. Cheverikin, D. Ivanov, A. Kondratiev, A. Dinsdale

Phase equilibria in the Fe-C-Ce system at 1100°C were studied using X-ray diffraction, SEM and electron probe microanalysis. An isothermal section at this temperature was constructed covering the whole concentration range.

The authors of the paper confirm that:

1. This manuscript is our original work and has not been published nor has it been submitted simultaneously elsewhere.
2. That all authors have checked the manuscript and have agreed to the submission.

Dear Dmitry G Eskin,

The authors are thankful to the reviewers for their thorough reviews and useful comments. The required corrections have been made in the revised paper.

Review of the paper "Phase equilibria in the Fe-Ce-C system at 1100°C"

(JALCOM-D-17-08498)

Reviewers' comments:

1. The composition found for the ternary phase should be included in the abstract.

The composition of the ternary phase is included.

2. The first sentence in the Introduction ("The introduction of rare-earth metals (R)...") makes no sense. It should be reformulated or deleted.

The first sentence has been deleted.

3. Section 3.2, last sentence: Does reference 14 contain a statement about CeC6?

The ref. has been corrected.

4. I could not find Ref. 27 in the text.

I have added a reference to ref 27 in the text.

Reviewer #2:

1. Cerium can react with O<sub>2</sub> in the air slowly. It is recommended that the authors re-analyze the samples including O<sub>2</sub>.

The samples have been melted in an arc furnace and kept in a protective atmosphere. A microstructure analysis of the samples was carried out directly after polishing the samples, so the samples did not have enough time to react with O<sub>2</sub>. In addition, we did not see any oxide phases on the microstructures or in the XRD results. This Explanation was added to section2.1.

2. The authors summarize the alloys data in Table 1. But the phase compositions were not given. On the other hand, from Fig.3a, it is not so convincing to conclude the existence of the CeC<sub>2</sub> phase. Considering these facts, the experimental results are quite questionable. The authors mentioned that EPMA determined carbon content is not reliable. However, the phase composition determination is critical for the construction of the Fe-Ce-C isothermal section at 1373 K. Thus, the authors should consider using other techniques to determine the phase compositions. By the way, the term "phase composition" used in this paper is wrong. The correct term is "phase identification".

We changed the term "phase composition" to "phase identification" in the manuscript as well as the Table 1 and added EPMA results.

Indeed, the amount of the CeC<sub>2</sub> phase in the sample Ce<sub>4</sub>Fe<sub>4</sub>C<sub>7</sub> is very low, so the peaks corresponding to this phase are barely noticeable. However, this phase is clearly visible on the microstructure of this sample. Therefore, we presented an additional X-ray diffraction pattern of the sample Ce<sub>3</sub>Fe<sub>5</sub>C<sub>6</sub> from the same three-phase region, on which peaks corresponding to the CeC<sub>2</sub> phase are clearly visible.

Unfortunately, the EDX analysis has its limitations. In order to decrease errors, which are inevitable during the measurement of carbide compositions, and increase the precision of the measurement, further calibrations using the carbides  $\text{Fe}_3\text{C}$ ,  $\text{Ce}_2\text{C}_3$  and  $\text{CeC}_2$  were carried out. However, the error of the carbon determination nevertheless exceeds the error of metal determination. But the fact that none of the phases show any variation of the lattice parameters indicates that the phases don't have any solubility of a third component. Therefore, the location of the three-phase regions cannot differ substantially from that shown in Fig. 1. In addition, the position of the three-phase regions was also determined by the ratio of phases in the two and three-phase alloys.

3. Page 3, last 4 line "Cooling of the alloys was performed with the furnace turned off". The reviewer really has concerns about this point. According to this sentence, furnace cooling was used. Please check carefully if this is true.

It has been corrected.

## Phase equilibria in the Fe-Ce-C system at 1100°C

M. Mardani<sup>1</sup>, I. Fartushna<sup>1</sup>, A. Khvan<sup>1</sup>, V. Cheverikin<sup>1</sup>, D. Ivanov<sup>1</sup>, A. Kondratiev<sup>1</sup>,  
A. Dinsdale<sup>2,3</sup>

<sup>1</sup> *Thermochemistry of Materials Scientific Research Centre, NUST MISIS,*

*Leninsky prosp. 4, 119049 Moscow, Russia*

<sup>2</sup> *Hampton Thermodynamics Ltd, UK*

<sup>3</sup> *BCAST, Brunel University London, Uxbridge, UK, UB8 2AD*

### Abstract

Phase equilibria in the Fe-Ce-C system at 1100°C were studied using X-ray diffraction, SEM and electron probe microanalysis. An isothermal section at this temperature was constructed covering the whole concentration range. The stability of the ternary compound  $\tau_1$  at 1100°C, identified previously, was confirmed and its composition determined as 23Fe-29Ce-48C according our data. It is also confirmed that the ternary compound  $\tau_1$  does not have a homogeneity range. The liquid phase is stable at 1100°C in the Fe-Ce-C system. The isothermal section is characterized by five three-phase regions:  $(\gamma\text{Fe}) + (\text{C}) + (\alpha\text{CeC}_2)$ ,  $(\gamma\text{Fe}) + \tau_1 + (\alpha\text{CeC}_2)$ ,  $(\gamma\text{Fe}) + \tau_1 + (\text{Ce}_2\text{C}_3)$ ,  $(\alpha\text{CeC}_2) + \tau_1 + (\text{Ce}_2\text{C}_3)$  and  $\text{L} + (\gamma\text{Fe}) + (\text{Ce}_2\text{C}_3)$  plus the corresponding two-phase regions.

*Keywords:* Phase diagram, ternary compound, isothermal section, Fe-Ce-C, rare earth metal, phase equilibria, lanthanides

\*Corresponding author.

*E-mail address:* [masuma.mardani@gmail.com](mailto:masuma.mardani@gmail.com)

## 1. Introduction

Rare-earth metals can be used to clean steels [1-3] and act as an inoculant in steels to form vermicular or nodular graphite. However, the mechanism of the influence of rare-earth additions on the properties of the steel is still not clear. Thus, an investigation of the phase equilibria in the Fe-Ce-C system is of great practical importance for the steel industry. In [4-7] it was reported that ternary compounds forming in Fe-R-C systems have been proposed as potential magnet materials.

Phase equilibria in the Fe-Ce-C system were studied experimentally by [8, 9]. Park et al. [8] investigated the Fe-Ce-C system in the composition range up to 40 at. % Ce and 60 at. % C on the basis of light microscopy and x-ray analysis of as-cast and annealed samples and provided a liquidus projection and isothermal sections at 800°C and 950°C, which were accepted later in the review of Raghavan [10] but redrawn to be compatible with the accepted binary data. Recently, we studied the phase equilibria in this system on crystallization using DTA, X-ray diffraction, SEM and electron probe microanalysis [9]. Liquidus and solidus projections for this system over the whole concentration range were constructed. This work is focused on an experimental study, using SEM, EPMA and X-ray diffraction, of phase equilibria in the Fe-Ce-C system at temperature of 1100°C.

### 1.2 Literature survey

#### *Binary systems*

The phase diagrams for the Ce-Fe and C-Fe binary systems from assessments [11] and [12], respectively are accepted and are in good agreement with all available experimental data. There are two stable intermetallic compounds in the Ce-Fe system,  $Ce_2Fe_{17}$  and  $CeFe_2$  (C15 Laves phase). The compound  $Ce_2Fe_{17}$  exists in two modifications, the temperature of the transformation is not known [13]. The high temperature modification ( $\beta Ce_2Fe_{17}$ ) has a rhombohedral  $Th_2Zn_{17}$ -type, while the low temperature modification ( $\alpha Ce_2Fe_{17}$ ) has a hexagonal  $Th_2Ni_{17}$ -type [13]. The solubilities of Ce in ( $\delta Fe$ ), ( $\gamma Fe$ ) and ( $\alpha Fe$ ) and Fe in ( $\delta Ce$ ) and ( $\gamma Ce$ ) are negligible. The assessment of data for the C-Fe system, carried out by Gustafson [12], is still widely used and is accepted in this work. Recently Naraghi et al. [14] also described this system; no significant changes in the phase equilibria at high temperature were made.

The binary C-Ce system adopted is based on the experimental work of [15]. The assessment [16] for this system did not include these experimental data. Two carbides form in this system,  $Ce_2C_3$  and  $CeC_2$ . The  $CeC_2$  carbide melts congruently at 2340°C and has two modifications. The high temperature modification ( $\beta CeC_2$ ) has a cubic  $CaF_2$ -type structure, while the low temperature modification ( $\alpha CeC_2$ ) has a tetragonal structure of the  $CaC_2$  type. The phase ( $\beta CeC_2$ ) has narrow homogeneity region. The solubilities of C in ( $\delta Ce$ ) and ( $\gamma Ce$ ) are ~10 at.%.

Bonhomme and Gosselin [17] also identified a compound  $CeC_6$ . However, the assessments [16, 18, 19] and the experimental work [8, 9, 15] did not include this compound.

### ***Ternary intermetallic compounds***

Park et al. [8] observed two intermetallic compounds  $Ce_4Fe_4C_7$  and  $Ce_2Fe_2C_3$  which form through solid state reactions. The formation temperature of the ternary compound  $Ce_4Fe_4C_7$  is above  $950^\circ C$  while the formation of the compound  $Ce_2Fe_2C_3$  has been reported to be between  $950$  and  $800^\circ C$  [8]. A compound  $Ce_4Fe_4C_7$  ( $\tau_1$ ) has also been reported by [20] although its composition is not known exactly. Mooij et al. [21] estimated this composition to be close to  $R_3Fe_5C_6$  ( $R = Ce, Pr, Nd, Sm$  and  $Gd$ ) and indicated that  $R_3Fe_5C_6$  is a refined composition of the previously reported compound  $R_4Fe_4C_7$  ( $R = Ce, Gd$ ) [8, 22].

The compounds reported with the tentative compositions  $Ce_{10}Fe_3C_{17}$  [23] and  $Ce_2Fe_2C_3$  [8] seem to be identical with the carbide  $Ce_{3.67}FeC_6$  [24]. Recently, in [25] the  $La_{3.67}[Fe(C_2)_3]$  compound with a structure  $P6_3/m$  was reinvestigated.

The compounds reported with the compositions  $R_3Fe_{20}C$  ( $R = La$  [23],  $Gd$  [22]) and  $R_{14}Fe_{78}C_8$  [26] seem to be identical with the composition  $R_2Fe_{14}C$  ( $Nd_2Fe_{14}B$ -structure type,  $P4_2/mnm$ ) [27]. In [6] it was demonstrated that  $Ce_2Fe_{14}C$  can be formed by the rapid solidification technique of melt spinning together with a comparatively brief heat treatment at an appropriate temperature.

## **2 Experimental**

### **2.1 Sample preparation**

The alloys were melted in an arc-furnace with a tungsten electrode on a water-cooled copper hearth in an Ar atmosphere 99.998% pure (pressure 80 kPa), purified by a Ti-melt with the purity of the starting materials, Fe-99.99%, C-99.8% and Ce-99.8%. To achieve homogeneity, the buttons were turned over and remelted six times. The weights of the ingots were typically 3 g. The weight losses did not exceed 0.1 %. So, generally the composition of the samples was taken according to their nominal composition.

The alloys were subjected to homogenization heat treatment at  $1100^\circ C$  for 24-85 hours. The annealing was performed in a tube furnace (Nabertherm RHTV 120/300/1700) with a temperature accuracy of  $\pm 3^\circ C$ . Annealing took place in an argon atmosphere 99.998% pure. The samples were placed in an  $Al_2O_3$  crucible. The samples were subjected to furnace cooling.

In order to preserve the samples, that show a tendency to disintegrate, the samples were kept in protective atmosphere and microstructure analysis of the samples was carried out directly after polishing the samples, so the samples did not have enough time to react with  $O_2$ . In addition, we did not see any oxide phases on the microstructures or in the XRD results.



X-ray diffraction (XRD), optical (OM), scanning electron microscopy (SEM), and electron microprobe analysis (EPMA) were used for investigation of this system.

## 2.2 Microstructure analysis

Metallographic specimens for microscopic examination were prepared by a Struers Labopol-5 machine. Firstly, the samples were ground using SiC-paper and then were polished with diamond discs with grain sizes of 9, 6, 3 and 1 microns. A diamond suspension was sprayed at regular intervals during the preparation. The microstructure of the alloys was examined using optical microscopy (OM) (Olympus-GX71F-5) and scanning electron microscopy (SEM) using a TESCAN VEGA LMH microscope with a LaB<sub>6</sub> cathode and an energy dispersive X-ray microanalysis system – Oxford Instruments Advanced AZtecEnergy. Both backscattered electron and secondary electron imaging were used in the analysis. An electron microprobe analysis (EPMA) was carried out on all phases using a four-crystal wave spectrometer (the analysed particle size was larger than 2 μm). The acceleration voltage used for the EPMA was 20 kV. The error of measurement in determining the concentration of elements using X-ray analysis was 0.2 wt.%. The detector was calibrated using standard samples of Co (99.99%), Cu (99.999%), Ni (99.99%), Mn (99.99%), Fe (99.999%), CeO<sub>2</sub> (99.99%), C (99.99%) and Cr (99.99%) from Oxford Instruments. In order to minimize errors, which are inevitable during measurement of carbide compositions, and increase the precision of the measurements, further calibrations using the carbides Fe<sub>3</sub>C, Ce<sub>2</sub>C<sub>3</sub> and CeC<sub>2</sub> were carried out.

## 2.3 X-ray diffraction analysis

X-ray diffraction (XRD) analysis was applied to determine the phase identification of the alloys using CuKα radiation operated at a voltage of 40 kV, a current of 40 mA and filtered with a Ni-crystal monochromator. XRD measurements were performed using a multipurpose X-ray diffractometer (Bruker-AXS D8 Discover). A parallel beam with a divergence of 0.03° is formed using the mirror of Gobel. The reflected intensity of the beam was measured using LYNXEYE position sensitive detector (angular resolution of 0.015°). Indexing of the reflections was performed with the WinXPOW and PowderCell software products.

## 3. Results and discussion

The alloys were studied after annealing at 1100°C for 24-85 hours. A complete list of investigated samples in this system, as well as the phase identification of the alloys and EPMA data is given in Table 1. An isothermal section of the Fe-Ce-C system at this temperature was constructed and shown in Fig. 1. The microstructures of some of the annealed samples are presented in Fig. 2. The lattice parameters of the solid phases are shown in Table 2.

### 3.1 The ternary compound $\tau_1$

The ternary compound  $\tau_1$  ( $\text{Nd}_3\text{Fe}_5\text{C}_6$ -type structure,  $P-4m2$ ,  $a = 7.231$ ,  $c = 3.192 \text{ \AA}$  [21]), which forms in solid state by peritectoid reaction  $(\gamma\text{Fe}) + \beta\text{CeC}_2 + \text{Ce}_2\text{C}_3 \rightleftharpoons \tau_1$ , was found to exist at a temperature of  $1100^\circ\text{C}$ . The ternary compound  $\tau_1$  at  $1100^\circ\text{C}$  does not show any variation of the lattice parameters on changes of composition, which indicates that  $\tau_1$  does not have a homogeneity range (Table 2).

The composition of  $\tau_1$  is not exactly known. The correct composition of the  $\tau_1$ -phase can be determined from EPMA. Unfortunately the quality of EPMA is moderate, and considerably exceeds the error of the carbon content determination, that is why the ratio of metallic contents Ce/Fe only was determined. Samples ## 8, 9, 12-16 were investigated using electron probe microanalysis and it was found that these alloys contain the ternary compound  $\tau_1$ , with a Ce/Fe ratio of 56/44. From the results of SEM, EPMA and XRD on the alloys #8 ( $\text{Ce}_4\text{Fe}_4\text{C}_7$ ) and #12 ( $\text{Ce}_3\text{Fe}_5\text{C}_6$ ), and the observation of additional phases ( $\gamma\text{Fe}$ ) and  $\alpha\text{CeC}_2$  in the sample #12 with the overall composition of ( $\text{Ce}_3\text{Fe}_5\text{C}_6$ ), it is confirmed that the composition of the  $\tau_1$ -phase is closer to the composition of  $\text{Ce}_4\text{Fe}_4\text{C}_7$ , than to  $\text{Ce}_3\text{Fe}_5\text{C}_6$  (Figs. 2 a, b, 3 a, b). In addition, the presence of phases ( $\gamma\text{Fe}$ ) and  $\alpha\text{CeC}_2$  in the alloy #8 indicate that the Ce content in the  $\tau_1$ -phase is a little higher than given by the stoichiometry  $\text{Ce}_4\text{Fe}_4\text{C}_7$ , while the Fe content in this phase is slightly lower. This was also observed in [20], the atom ratio in  $\tau_1$ -phase is Ce:Fe:C = 4.4:4:7.2. Thus, according to our data the composition of  $\tau_1$  is 23Fe-29Ce-48C.

The crystal structure of the ternary compound  $\tau_1$  is not completely resolved. Park et al. [8] determined that the compound  $\text{Ce}_4\text{Fe}_4\text{C}_7$  ( $\tau_1$ ) had a primitive tetragonal structure ( $tP^*$ ,  $a = 7.22$ ,  $c = 5.82 \text{ \AA}$ ). Mooij et al. [21] attempted to find a crystal structure for this phase and provide a possible model for filling a unit cell with heavy atoms on the basis of a  $\text{Nd}_3\text{Fe}_5\text{C}_6$ -type structure, ( $P-4m2$ ,  $a = 7.231$ ,  $c = 3.192 \text{ \AA}$ ). However, the crystal structure has not been resolved completely yet. It should be noted that some unexplained reflection lines are present in the X-ray patterns of the samples ##8, 11-13 (Fig. 3 a).

In order to check the existence of other ternary compounds in the Fe-Ce-C system at  $1100^\circ\text{C}$ , we prepared several alloys with the compositions of possible ternary compounds which had been found in Fe-R-C systems.

The ternary compound  $\text{Ce}_{3.67}\text{FeC}_6$  ( $\tau_2$ ) (# 16) [24, 25] which had been identified by [8] with the tentative composition  $\text{Ce}_2\text{Fe}_2\text{C}_3$  (# 9) was not observed by us in the annealed alloys at  $1100^\circ\text{C}$ . This confirms that the ternary compound  $\tau_2$  forms through a peritectoid reaction  $(\gamma\text{Fe}) + \text{Ce}_2\text{C}_3 \rightleftharpoons \tau_2$  at a temperature between  $950$  and  $800^\circ\text{C}$  [8].

The ternary compound with the composition of  $RFeC_2$  (ScCoC<sub>2</sub>-type structure, *tP8-P4/nmm* and CeNiC<sub>2</sub>-type structure, *oS8-Amm2*) which had been found in systems with R = Sc, Y, Sm, Gd-Er and Lu [21, 29-32], was not found in Fe-Ce-C system. However, the general view of microstructure of alloy # 11 with composition CeFeC<sub>2</sub> reveals a small amount of the  $\tau_1$ -phase and existence of ( $\gamma$ Fe) and  $\alpha$ CeC<sub>2</sub>. This gives us reason to believe that the composition of alloy # 11 is almost on the boundary tie-line ( $\gamma$ Fe) +  $\alpha$ CeC<sub>2</sub>. Alloy #10 with composition Ce<sub>3</sub>Fe<sub>2</sub>C<sub>6</sub> has been shown to contain two-phases ( $\gamma$ Fe) +  $\alpha$ CeC<sub>2</sub>. It should be noted that the ternary compound R<sub>3</sub>Fe<sub>2</sub>C<sub>6</sub>, of unknown crystal structure, was found only in the system with Dy at 800°C [28]. In [33] the existence of a compound close to the composition R<sub>2</sub>FeC<sub>4</sub> with an orthorhombic crystal structure (Er<sub>2</sub>FeC<sub>4</sub>-type structure, *oI28-Ibam*) for R = Y, Tb-Lu was reported, we did not observe this compound in Fe-Ce-C system at 1100°C.

Another ternary compound with composition R<sub>11</sub>Fe<sub>12</sub>C<sub>18</sub>, which was found in the system with Sm (Th<sub>11</sub>Ru<sub>12</sub>C<sub>18</sub>-type structure, *cI82-I-43m*) [34], does not form at 1100°C in the Fe-Ce-C system, based on the SEM, EPMA and XRD results on alloy # 13 with the composition Ce<sub>11</sub>Fe<sub>12</sub>C<sub>18</sub>. This alloy contains the three phases  $\tau_1$  + ( $\gamma$ Fe) + Ce<sub>2</sub>C<sub>3</sub>, the amount of  $\tau_1$ -phase in this alloy being very high (Figs. 2 c, 3 c), and consequently, the alloy is located close to the composition of the ternary compound  $\tau_1$ . This further proves that the composition of  $\tau_1$ -phase is closer to the composition of Ce<sub>4</sub>Fe<sub>4</sub>C<sub>7</sub>, than to Ce<sub>3</sub>Fe<sub>5</sub>C<sub>6</sub>.

The novel intermediate ternary phases R<sub>15</sub>Fe<sub>8</sub>C<sub>25</sub> (R = Y, Dy, Ho, Er) (Er<sub>15</sub>Fe<sub>8</sub>C<sub>25</sub>-type structure, *hP49-P321*) have been identified by [28, 35, 36]. The alloy # 14 with the composition Ce<sub>15</sub>Fe<sub>8</sub>C<sub>25</sub> contains only phases  $\tau_1$  + Ce<sub>2</sub>C<sub>3</sub> +  $\alpha$ CeC<sub>2</sub> (Fig. 2 d). In [36] the ternary phase R<sub>5,64</sub>Fe<sub>2</sub>C<sub>9</sub> (R = Y, Gd, Tb, Dy) with an orthorhombic crystal structure *Pnma* also has been reported. We did not observe this phase in Fe-Ce-C system. It is most likely that these compounds form only in R-Fe-C systems with heavy rare-earth metals.

Therefore, no other ternary compounds, besides  $\tau_1$ , were identified in the Fe-Ce-C system at a temperature of 1100°C

### 3.2 Phase equilibria

At the temperature of 1100°C,  $\tau_1$  is in equilibrium with the phases ( $\gamma$ Fe), ( $\alpha$ CeC<sub>2</sub>) and (Ce<sub>2</sub>C<sub>3</sub>) forming three, three-phase fields, namely ( $\gamma$ Fe) +  $\tau_1$  + ( $\alpha$ CeC<sub>2</sub>), ( $\gamma$ Fe) +  $\tau_1$  + (Ce<sub>2</sub>C<sub>3</sub>), ( $\alpha$ CeC<sub>2</sub>) +  $\tau_1$  + (Ce<sub>2</sub>C<sub>3</sub>), and the corresponding two-phase regions. In addition, two more three phase regions, ( $\gamma$ Fe) + (C) + ( $\alpha$ CeC<sub>2</sub>) and L + ( $\gamma$ Fe) + (Ce<sub>2</sub>C<sub>3</sub>) are present in the phase diagram at this temperature (Fig. 1).

The microstructure results of the alloys ## 8, 11 and 12 clearly show three distinct phases: black grains, a grey matrix and dark-grey grains (Fig. 2 a, b) which correspond to ( $\gamma$ Fe),

$\tau_1$  and ( $\alpha\text{CeC}_2$ ), respectively and this is confirmed by XRD data (Figs. 3 *a, b*). Therefore these samples are located in the ( $\gamma\text{Fe}$ ) +  $\tau_1$  + ( $\alpha\text{CeC}_2$ ) three-phase region

In the SEM micrograph and the X-Ray of samples #9 and #13, three phases,  $\tau_1$  (light-grey matrix) + ( $\gamma\text{Fe}$ ) (grey grains) + ( $\text{Ce}_2\text{C}_3$ ) (white grains), are well distinguished (Figs. 1, 2 *c, 3 c*, Tables 1-2). The amount of the  $\tau_1$ -phase in the alloy #13 is very high and, consequently, the alloy is located close to the composition of the ternary compound  $\tau_1$ . On the other hand the amount of  $\text{Ce}_2\text{C}_3$  is very low and, therefore, the composition of this alloy is almost on the boundary tie-line  $\tau_1$  + ( $\gamma\text{Fe}$ ).

Moreover, another three-phase region involving the  $\tau_1$ -phase is formed in the Fe-Ce-C system at 1100°C. It was determined with SEM, EMPA and XRD of the three-phase alloys ## 14-16, which contain the three phases ( $\alpha\text{CeC}_2$ ) (grey grains) +  $\tau_1$  (light-grey matrix) + ( $\text{Ce}_2\text{C}_3$ ) (white grains) (Tables 1-2, Figs. 1, 2 *d*).

The location of the three-phase region ( $\gamma\text{Fe}$ ) + (C) + ( $\alpha\text{CeC}_2$ ) was established based on the results for alloys #4, 5 and 7 with three phases in equilibrium (Figs. 2 *e, 3 d*) and alloys ##1, 3 and 10 with the two-phases ( $\gamma\text{Fe}$ ) + ( $\alpha\text{CeC}_2$ ) in equilibrium (Tables 1-2, Fig. 1).

The location of the liquid phase was determined by the construction and processing of a series of intersecting isopleths. A three-phase region involving the liquid phase, L + ( $\gamma\text{Fe}$ ) + ( $\text{Ce}_2\text{C}_3$ ), is present. The isopleths were used to refine the location of this three-phase region containing the liquid-phase.

No binary intermetallic phases have appreciable solubility of the third component. The  $\text{CeC}_6$  compound reported in [17] was not found by us in the ternary Fe-Ce-C system at 1100°C.

#### 4. Conclusions

Phase equilibria in the Fe-Ce-C system at 1100°C were studied over the whole concentration region. An isothermal section at this temperature was constructed. The ternary compound  $\tau_1$  is stable at this temperature and is in equilibrium with the phases ( $\gamma\text{Fe}$ ), ( $\alpha\text{CeC}_2$ ) and ( $\text{Ce}_2\text{C}_3$ ). No binary intermetallic phases have appreciable solubility of the third component.

#### Acknowledgments:

This work was carried out with financial support from the Ministry of Education and Science of the Russian Federation in the framework of the basic part of the state program ‘Organisation of the Research Work’ for higher educational institutions in 2017–2019.

## References

- [1] L. Wang, Q. Lin, J. Ji, D. Lan, New study concerning development of application of rare earth metals in steels, *Journal of Alloys and Compounds* 408-412 (2006) 384-386.
- [2] Y. Jun, D. Zou, X. Li, Z. Du, Effect of rare earth on microstructures and properties of high speed steel with high carbon content, *Journal of Iron and Steel Research, International* 14(1) (2007) 47-52, 59.
- [3] N. Lin, F. Xei, T. Zhong, X. Wu, W. Tian, Influence of adding various rare earths on microstructures and corrosion resistance of chromizing coatings prepared via pack cementation on P110 steel, *J. Rare Earths* 28 (2010) 301-304.
- [4] D.B. De Mooij, K.H.J. Buschow, Formation and magnetic properties of the compounds  $R_2Fe_{14}C$ , *Journal of the Less Common Metals* 142 (1988) 349-357.
- [5] K.H.J. Buschow, D.B. De Mooij, C.J.M. Denissen, Note on the formation and the magnetic properties of the compound  $Nd_2Fe_{14}C$ , *Journal of the Less Common Metals* 141(1) (1988) L15-L18.
- [6] C.D. Fuerst, J.F. Herbst, Formation of  $R_2Fe_{14}C$  compounds ( $R = Y, Ce$ ) by rapid solidification, *Journal of applied physics* 69(11) (1991) 7727-7730.
- [7] E. Burzo, Permanent magnets based on R-Fe-B and R-Fe-C alloys, *Reports on Progress in Physics* 61(9) (1998) 1099-1266.
- [8] H.K. Park, H.H. Stadelmaier, L.T. Jordan, The ternary system iron-cerium-carbon, *Zeitschrift für Metallkunde* 73(6) (1982) 399-402.
- [9] A.V. Khvan, I.V. Fartushna, M. Mardani, A.T. Dinsdale, V.V. Cheverikin, An experimental investigation of the liquidus projection in the Fe-Ce-C system, *Journal of Alloys and Compounds* 651 (2015) 350-356.
- [10] V. Raghavan, The C-Ce-Fe (carbon–cerium–iron) system, *Phase diagrams ternary iron alloys*, *Indian Inst. Met.* 6 (1992) 489-495.
- [11] X. Su, J.-C. Tedenac, Thermodynamic modeling of the ternary Ce-Fe-Sb system: Assessment of the Ce–Sb and Ce–Fe systems, *Calphad* 30(4) (2006) 455-460.
- [12] P.A. Gustafson, Thermodynamic Evaluation of the Fe-C System, *Scand. J. Metall.* 14(5) (1985) 259-267.
- [13] K.H.J. Buschow, J.S van Wieringen, Crystal structure and magnetic properties of cerium-iron compounds, *Physica Status Solidi (b)* 42(1) (1970) 231-239.

- [14] R. Naraghi, M. Selleby, J. Ågren, Thermodynamics of stable and metastable structures in Fe-C system, *Calphad* 46 (2014) 148-158.
- [15] V.N. Eremenko, T.Y. Velikanova, O.V. Gordiychuk, Carbides of the Rare Earth Metals, Diagrams of the Systems RE-C, Kiev, Naukova Dumka (1992) 1-160 (in Russian).
- [16] Y. Peng, Y. Du, L. Zhang, C. Sha, S. Liu, F. Zheng, D. Zhao, X. Yuan, L. Chen, Thermodynamic modeling of the C-RE (RE = La, Ce and Pr) systems, *Calphad* 35(4) (2011) 533-541.
- [17] F. Bonhomme, P.A. Gosselin, Crystal Chemical Investigation of the System Ce-B-C, Thesis, INSA, Rennes, France (1988) 1-80 (in French).
- [18] K.A. Gschneidner, F.W. Calderwood, The C-Ce (Carbon-Cerium) system, *Bulletin of Alloy Phase Diagrams* 7(5) (1986) 437-438.
- [19] Gmelin Handbook of Inorganic Chemistry 8th Edition, Vol. C12a, Rare Earth Elements; Compounds with Carbon, Springer, Berlin (1995).
- [20] J.Z. Zhang, D.Z. Li, Thermodynamics of cerium carbide  $\text{Fe}_4\text{Ce}_4\text{C}_7$  in steel, *Acta Metallurgica Sinica (English Letters)* 11(2) (1998) 150-156.
- [21] D.M. De Mooij, T.H. Jacobs, H.A.A. Keetels, J. Eisses, Nd-Fe-C compounds; phase relations and magnetic properties, Philips Nat. Lab. Unclass. Rep. 005/90, Eindhoven (1990) 28.
- [22] H.H. Stadelmaier, K.P. Hee, The system iron-gadolinium-carbon and its ternary carbides, *Zeitschrift fuer Metallkunde* 72(6) (1981) 417-422.
- [23] E.P. Marusin, The ternary {Y, La, Ce}-Fe-C systems, Dep. Doc, SPSTL 369, Khp, D82. (1982) 1-6 (in Russian).
- [24] A.M. Witte, W. Jeitschko, Preparation and Crystal Structure of the Isotypic Carbides  $\text{Ln}_{3.67}\text{TC}_6$  (Ln = rare earth elements; T = Mn, Fe, Ru) and  $\text{Eu}_{3.16}\text{NiC}_6$ , *Zeitschrift für Naturforschung B* 51 (2) (1996) 249-256.
- [25] B. Davaasuren, E. Dashjav, G. Kreiner, H. Borrmann, R. Kniep, Reinvestigation and superstructure of  $\text{La}_{3.67}[\text{Fe}(\text{C}_2)_3]$ , *Journal of Solid State Chemistry* 182(6) (2009) 1331-1335.
- [26] F. Xing, W. Ho, Crystallographic and magnetic behaviors of the R-Fe-C compounds, *Journal of Applied Physics* 67(9) (1990) 4604-4606.
- [27] E.P. Marusin, O.I. Bodak, A.O. Tsokol, V.S. Fundamenskii, Crystal structure of the  $\text{La}_2\text{Fe}_{14}\text{C}$  compound, *Kristallografiya* 30(3) (1985) 581-583 (in Russian).
- [28] V.O. Levytskyy, Compounds of the R-M-C systems (R = RE, M = 3d-element) and their hydrides: synthesis, structure and properties, Thesis (2015) 159 (in Ukrainian).
- [29] E.P. Marusin, O.I. Bodak, A.O. Tsokol, M.G. Bayvelman, Crystal structure of the  $\text{ScMC}_2$  (M = Fe, Co, Ni) compounds, *Kristallografiya* 30(3) (1985) 584-586 (in Russian).

- [30] N.A. El-Masry, H.H. Stadelmaier, The ternary system Iron-Yttrium-Carbon, *Zeitschrift für Metallkunde* 80 (1989) 723-725.
- [31] W. Jeitschko, M.H. Gerss, Ternary carbides of the rare earth and iron group metals with CeCoC<sub>2</sub>- and CeNiC<sub>2</sub>-type structure, *Journal of the Less-Common Metals* 116 (1986) 147-157.
- [32] R. Pöttgen, W. Jeitschko, U. Wortmann, M.E. Danebrock, Crystal structures and physical properties of the ternary carbides ScT<sub>1-x</sub>C<sub>2</sub>, (T = Fe, Co, Ni), *Journal of Materials Chemistry* 2(6) (1992) 633-637.
- [33] M.H. Gerss, W. Jeitschko, L. Boonk, J. Nientiedt, J. Grobe, E. Mörsen, A. Leson, Preparation and Crystal Structure of Superconducting Y<sub>2</sub>FeC<sub>4</sub> and Isotypic Lanthanoid Iron Carbides, *Journal of Solid State Chemistry* 70 (1987) 19-28.
- [34] A.A. Putyatin, S.N. Nesterenko, Crystal structure model of Sm<sub>11</sub>Fe<sub>12</sub>C<sub>18</sub>, *Soviet Physics Crystallography* 37 (1992) 111-112 (translated from *Kristallografiya*).
- [35] B. Davaasuren, H. Borrmann, E. Dashjav, G. Kreiner, M. Widom, W. Schnelle, R. Wagner, R. Kniep, Planar Fe<sub>6</sub> cluster units in the crystal structure of RE<sub>15</sub>Fe<sub>8</sub>C<sub>25</sub> (RE = Y, Dy, Ho, Er), *Angew. Chem.* 122 (2010) 5824-5828.
- [36] B. Davaasuren, Carbometalates: Intermediate phases in the ternary systems RE-T-C (RE = Y, La, Gd-Er; T = Cr, Fe, Ru), Thesis, Technische Universität Dresden (2010) 197.
- [37] T.B. Massalski, (Ed), *Binary Alloy Phase Diagrams*, 2nd Edition, ASM International, Metals Park, OH, 1990.
- [38] Y.C. Chuang, C.H. Wu, Z.B. Shao, Investigation of the Ce-Fe binary system, *Journal of the Less Common Metals* 136(1) (1987) 147-153.
- [39] Z. Altounian, X. Chen, L.X. Liao, D.H. Ryan, J.O. Ström-Olsen, Structure and magnetic properties of rare-earth iron nitrides, carbides and carbonitrides, *Journal of applied physics* 73(10) (1993) 6017-6022.
- [40] H. Sun, Y. Otani, J.M.D. Coey, Gas-phase carbonation of R<sub>2</sub>Fe<sub>17</sub>, *Journal of Magnetism and Magnetic Materials* 104-107 (1992) 1439-1440.
- [41] X.P. Zhong, R.J. Radwański, F.R. De Boer, T.H. Jacobs, K.H.J. Buschow, Magnetic and crystallographic characteristics of rare-earth ternary carbides derived from R<sub>2</sub>Fe<sub>17</sub> compounds, *Journal of Magnetism and Magnetic Materials* 86(2-3) 333-340.
- [42] M. Gueramian, A. Bezinge, K. Yvon, J. Muller, Synthesis and magnetic properties of ternary carbides R<sub>2</sub>Fe<sub>14</sub>C (R = Pr, Sm, Gd, Tb, Dy, Ho, Er, Tm, Lu) with Nd<sub>2</sub>Fe<sub>14</sub>B structure type, *Solid state communications* 64(5) (1987) 639-644.
- [43] L.X. Liao, X. Chen, Z. Altounian, D.H. Ryan, Structure and magnetic properties of R<sub>2</sub>Fe<sub>17</sub>C<sub>x</sub> (x~2.5), *Applied physics letters* 60(1) (1992) 129-131.
- [44] N.H. Duc, T.D. Hien, Magnetic properties of (Ce,R)(Fe,Al)<sub>2</sub> compounds, *J. Magnetism and*

Magnetic Materials 140-144 (1995) 1113-1114.

[45] C.D. Fuerst, J.F. Herbst, Formation of  $R_2Fe_{14}C$  compounds ( $R = Y, Ce$ ) by rapid solidification, Journal of applied physics 69(11) (1991) 7727-7730.



### Figure captions

Fig. 1. The isothermal section at 1100°C of the Fe-Ce-C system: ● – two-phase samples; ● – three-phase samples.

Fig. 2. Microstructure of annealed samples at 1100°C of alloys in the Fe-Ce-C system:

- a –  $\text{Ce}_4\text{Fe}_4\text{C}_7$  (#8),  $\times 2000$ ,  $\tau_1 + (\gamma\text{Fe}) + (\alpha\text{CeC}_2)$ ;
- b –  $\text{Ce}_3\text{Fe}_5\text{C}_6$  (#12),  $\times 2000$ ,  $\tau_1 + (\gamma\text{Fe}) + (\alpha\text{CeC}_2)$ ;
- c –  $\text{Ce}_{11}\text{Fe}_{12}\text{C}_{18}$  (#13),  $\times 2000$ ,  $\tau_1 + (\gamma\text{Fe}) + (\text{Ce}_2\text{C}_3)$ ;
- d –  $\text{Ce}_{15}\text{Fe}_8\text{C}_{25}$  (#14),  $\times 2000$ ,  $\tau_1 + (\alpha\text{CeC}_2) + (\text{Ce}_2\text{C}_3)$ ;
- e – 60Fe-10Ce-30C (#4),  $\times 1000$ ,  $(\gamma\text{Fe}) + (\alpha\text{CeC}_2) + (\text{C})$ .

Fig. 3. X-ray diffraction patterns of annealed alloys in the Fe-Ce-C system:

- a –  $\text{Ce}_4\text{Fe}_4\text{C}_7$  (#8),  $\tau_1 + (\gamma\text{Fe}) + (\alpha\text{CeC}_2)$ ;
- b –  $\text{Ce}_3\text{Fe}_5\text{C}_6$  (#12),  $\tau_1 + (\gamma\text{Fe}) + (\alpha\text{CeC}_2)$ ;
- c –  $\text{Ce}_{11}\text{Fe}_{12}\text{C}_{18}$  (#13),  $\tau_1 + (\gamma\text{Fe}) + (\text{Ce}_2\text{C}_3)$ ;
- d – 60Fe-10Ce-30C (#4),  $(\gamma\text{Fe}) + (\alpha\text{CeC}_2) + (\text{C})$ .

Phase equilibria in the Fe-Ce-C system at 1100°C were studied.

An isothermal section at this temperature was constructed.

The ternary compound  $\tau_1$  is stable at this temperature.

Compositionn of  $\tau_1$  determined as 23Fe-29Ce-48C according our data

Table 1. Phase identification and composition of the Fe-Ce-C phases according to the EPMA examination of annealed at 1100°C for 24-85 h alloys

#	Alloy, at.%			Heat-treatment	Phase identification	Microprobe results, at.% <sup>1</sup>		
	Fe	Ce	C			Phase	Fe	Ce
1	87	2	11	1100°C, 35 h	$\tau_1 + (\alpha\text{CeC}_2)$	-	-	-
2	85	4	11	1100°C, 85 h	$\tau_1 + (\alpha\text{CeC}_2) + (\gamma\text{Fe})$	-	-	-
3	80	5	15	1100°C, 85 h	$\tau_1 + (\alpha\text{CeC}_2)$	-	-	-
4	60	10	30	1100°C, 24 h	$(\gamma\text{Fe}) + (\alpha\text{CeC}_2) + (\text{C})$	( $\gamma\text{Fe}$ )	99.4±0.1	0.6±0.1
						(C)	0.0±0.0	0.0±0.0
5	45	15	40	1100°C, 24 h	$(\gamma\text{Fe}) + (\alpha\text{CeC}_2) + (\text{C})$	( $\gamma\text{Fe}$ )	99.3±0.1	0.7±0.1
						(C)	0.0±0.0	0.0±0.0
6	60	16	24	1100°C, 35 h	$(\gamma\text{Fe}) + (\text{Ce}_2\text{C}_3)$	-	-	-
7	15	25	60	1100°C, 24 h	$(\gamma\text{Fe}) + (\alpha\text{CeC}_2) + (\text{C})$	-	-	-
8	26.7	26.7	46.6	1100°C, 24 h	$\tau_1 + (\alpha\text{CeC}_2) + (\gamma\text{Fe})$	$\tau_1$	44.1±0.1	55.9±0.1
						( $\gamma\text{Fe}$ )	98.5±0.1	1.5±0.1
9	28.6	28.6	42.8	1100°C, 24 h	$\tau_1 + (\text{Ce}_2\text{C}_3) + (\gamma\text{Fe})$	$\tau_1$	43.8±0.3	56.2±0.3
						( $\gamma\text{Fe}$ )	98.6±0.1	1.4±0.1
10	18.2	27.3	54.5	1100°C, 35 h	$(\alpha\text{CeC}_2) + (\gamma\text{Fe})$	( $\alpha\text{CeC}_2$ )	0.5±0.3	99.5±0.3
11	25	25	50	1100°C, 35 h	$(\alpha\text{CeC}_2) + (\gamma\text{Fe})$	-	-	-
12	35.7	21.4	42.9	1100°C, 35 h	$\tau_1 + (\alpha\text{CeC}_2) + (\gamma\text{Fe})$	$\tau_1$	44.1	55.9
						( $\alpha\text{CeC}_2$ )	1.1	98.9
13	29.3	26.8	43.9	1100°C, 35 h	$\tau_1 + (\text{Ce}_2\text{C}_3) + (\gamma\text{Fe})$	$\tau_1$	44.0±0.1	56.0±0.1
14	16.7	31.2	52.1	1100°C, 35 h	$\tau_1 + (\alpha\text{CeC}_2) + (\text{Ce}_2\text{C}_3)$	$\tau_1$	43.8±0.1	56.2±0.0
						( $\text{Ce}_2\text{C}_3$ )	0.5±0.1	99.5±0.1
15	10	33	57	1100°C, 35 h	$\tau_1 + (\alpha\text{CeC}_2) + (\text{Ce}_2\text{C}_3)$	$\tau_1$	44.0±0.0	56.0±0.1
						( $\text{Ce}_2\text{C}_3$ )	0.4±0.1	99.6±0.1
16	9.4	34.4	56.2	1100°C, 35 h	$\tau_1 + (\alpha\text{CeC}_2) + (\text{Ce}_2\text{C}_3)$	-	-	-

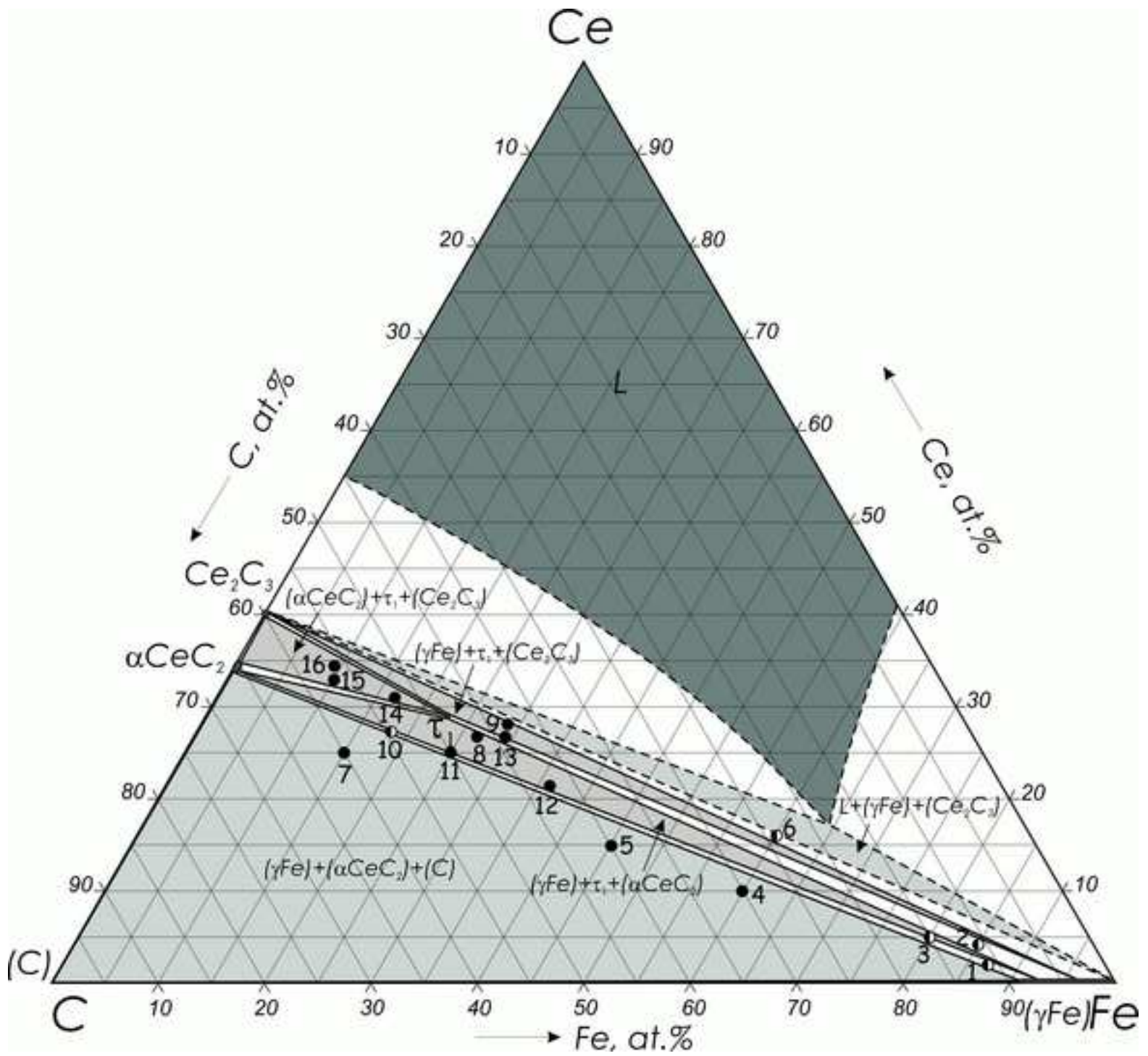
<sup>1</sup> The ratio of metal contents Fe/Ce was determined for the phases, since the error of the carbon content determination exceeds the error of the metal determination

Table 2. The crystal structures and lattice parameters of the Fe-Ce-C phases

Phase	Crystal structure	Lattice parameters, Å	Alloy	Refs.
$\delta$ Fe	W, <i>A2, cI2-Im3m</i>	$a = 2.9315$	-	[37]
$\gamma$ Fe	Cu, <i>A1, cF4-Fm-3m</i>	$a = 3.6467$	at 915°C	[37]
$\alpha$ Fe	W, <i>A2, cI2-Im3m</i>	$a = 2.8665$	at 25°C	[37]
		$a = 2.863(2)$	60Fe-30Ce-10C, 1100°C / 24 h	Th. w.
		$a = 2.866(1)$	Ce <sub>4</sub> Fe <sub>4</sub> C <sub>7</sub> (#8), 1100°C / 24 h	Th. w.
		$a = 2.865(2)$	Ce <sub>2</sub> Fe <sub>2</sub> C <sub>3</sub> (#9), 1100°C / 24 h	Th. w.
$\varepsilon$ Fe	Mg, <i>A3, hP2-P6<sub>3</sub>/mmc</i>	$a = 4.68, c = 3.96$	at 25°C, 13 GPa	[37]
$\delta$ Ce	W, <i>A2, cI2-Im3m</i>	$a = 4.12$	-	[37]
$\gamma$ Ce	Cu, <i>A1, cF4-Fm-3m</i>	$a = 5.1610$	-	[37]
$\beta$ Ce	$\alpha$ La, <i>A3', hP4-P6<sub>3</sub>/mmc</i>	$a = 3.6810, c = 11.857$	-	[37]
$\alpha$ Ce	Cu, <i>A1, cF4-Fm-3m</i>	$a = 4.85$	-	[37]
(C)	C-graphite, <i>A9, hP4-P6<sub>3</sub>/mmc</i>	$a = 2.4612, c = 6.7090$	-	[37]
Fe <sub>17</sub> Ce <sub>2</sub> ht	Zn <sub>17</sub> Th <sub>2</sub> , <i>hR57-R-3m</i>	$a = 8.485, c = 12.433$	-	[38]
		$a = 8.496, c = 12.414$	-	[3]
Fe <sub>17</sub> Ce <sub>2</sub> C <sub>x</sub>	Pr <sub>2</sub> Mn <sub>17</sub> C <sub>1.77</sub> , <i>hR66-R-3m</i>	$a = 8.72, c = 12.64$	1170 K / week	[39]
		$a = 8.73, c = 12.56$	-	[40]
		$a = 8.540, c = 12.424$	1100°C / several weeks	[41]
		$a = 8.534, c = 12.436$	1170 K / 20-30 days	[42]
		$a = 8.74, c = 12.65$	x=2.8	[43]
Fe <sub>17</sub> Ce <sub>2</sub> rt	Th <sub>2</sub> Ni <sub>17</sub> , <i>hP38-P6<sub>3</sub>/mmc</i>	$a = 8.49, c = 8.281$	-	[13]
Fe <sub>2</sub> Ce	MgCu <sub>2</sub> , <i>C15, cF24-Fd-3m</i>	$a = 7.296$	-	[38]
		$a = 7.302$	-	[44]
Ce <sub>2</sub> C <sub>3</sub>	Pu <sub>2</sub> C <sub>3</sub> , <i>D5<sub>c</sub>, cI40-I-43d</i>	$a = 8.4480$	Ce-rich	[15]
		$a = 8.450$	C-rich	[15]
		$a = 8.446(1)$	Ce <sub>2</sub> Fe <sub>2</sub> C <sub>3</sub> C (#9), 1100°C / 24 h	Th. w.
$\beta$ CeC <sub>2</sub>	CaF <sub>2</sub> , <i>C1, cF12-Fm-3m</i>	$a = 5.939$	-	[15]
		$a = 5.927$	at 1110°C	[19]
		$a = 6.025$	at 2000°C	[19]
$\alpha$ CeC <sub>2</sub>	CaC <sub>2</sub> , <i>C11<sub>a</sub>, tI6-I<sub>4</sub>/mmm</i>	$a = 3.877(1), c = 6.485(2)$	-	[18]
		$a = 3.875, c = 6.489$	at 580°C, in equil. with Ce <sub>2</sub> C <sub>3</sub>	[15]
		$a = 3.878(1), c = 6.489(2)$	60Fe-30Ce-10C (#4), 1100°C / 24 h	Th. w.
CeC <sub>6</sub>	<i>hP14 (?) - P6<sub>3</sub>/mmc</i>	$a = 4.490, c = 13.9526$	-	[17]
Ce <sub>4</sub> Fe <sub>4</sub> C <sub>7</sub> (Ce <sub>3</sub> Fe <sub>5</sub> C <sub>6</sub> )	<i>tP*</i> Nd <sub>3</sub> Fe <sub>5</sub> C <sub>6</sub> , <i>P-4m2</i>	$a = 7.22, c = 5.82$	Ce <sub>4</sub> Fe <sub>4</sub> C <sub>7</sub> , 800°C / 300 h	[8]
		$a = 7.231, c = 3.192$	Ce <sub>3</sub> Fe <sub>5</sub> C <sub>6</sub> , 1050°C	[21]
		$a = 7.232(2), c = 3.192(1)$	Ce <sub>4</sub> Fe <sub>4</sub> C <sub>7</sub> (#8), 1100°C / 24 h	Th. w.
		$a = 7.231(2), c = 3.191(2)$	Ce <sub>2</sub> Fe <sub>2</sub> C <sub>3</sub> (#9), 1100°C / 24 h	Th. w.
		$a = 7.235(3), c = 3.194(2)$	Ce <sub>3</sub> Fe <sub>5</sub> C <sub>6</sub> (#12), 1100°C / 35 h	Th. w.
Ce <sub>3.67</sub> FeC <sub>6</sub> (Ce <sub>2</sub> Fe <sub>2</sub> C <sub>3</sub> )	La <sub>3.67</sub> FeC <sub>6</sub> , <i>hP24-P6<sub>3</sub>/m</i>	$a = 8.686, c = 5.309$	800-1000°C / 5-9 weeks	[37]
		$a = 8.7926(8),$ $c = 16.0459(15)$	for La <sub>3.67</sub> FeC <sub>6</sub>	[38]
Ce <sub>2</sub> Fe <sub>14</sub> C	Nd <sub>2</sub> Fe <sub>14</sub> B, <i>tP68-P4<sub>2</sub>/mnm</i>	$a = 8.74, c = 11.85$	annealed at 970 K / 0.5 h	[45]

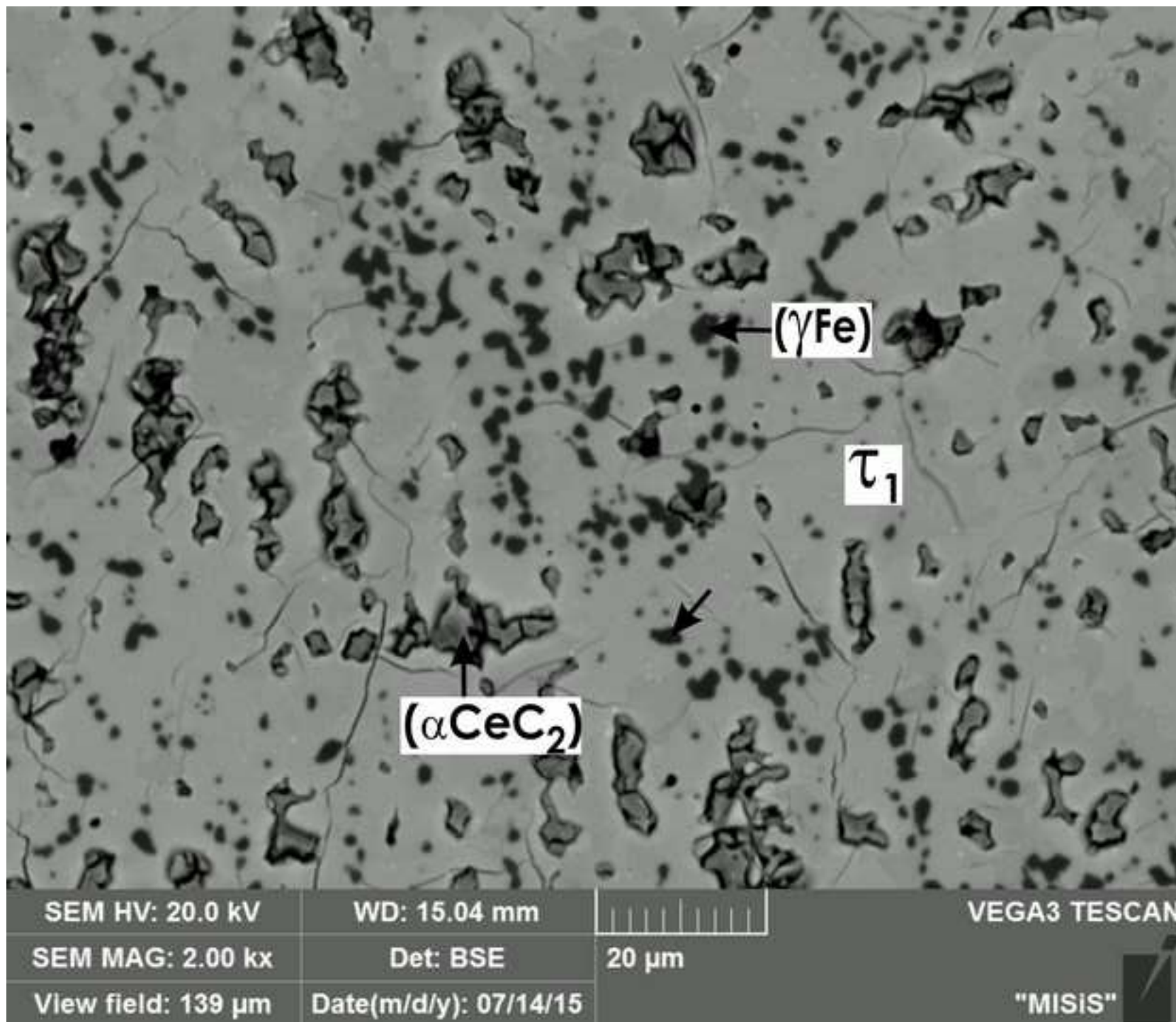
<sup>1</sup> Th. w. – results of this work

Figure  
[Click here to download high resolution image](#)



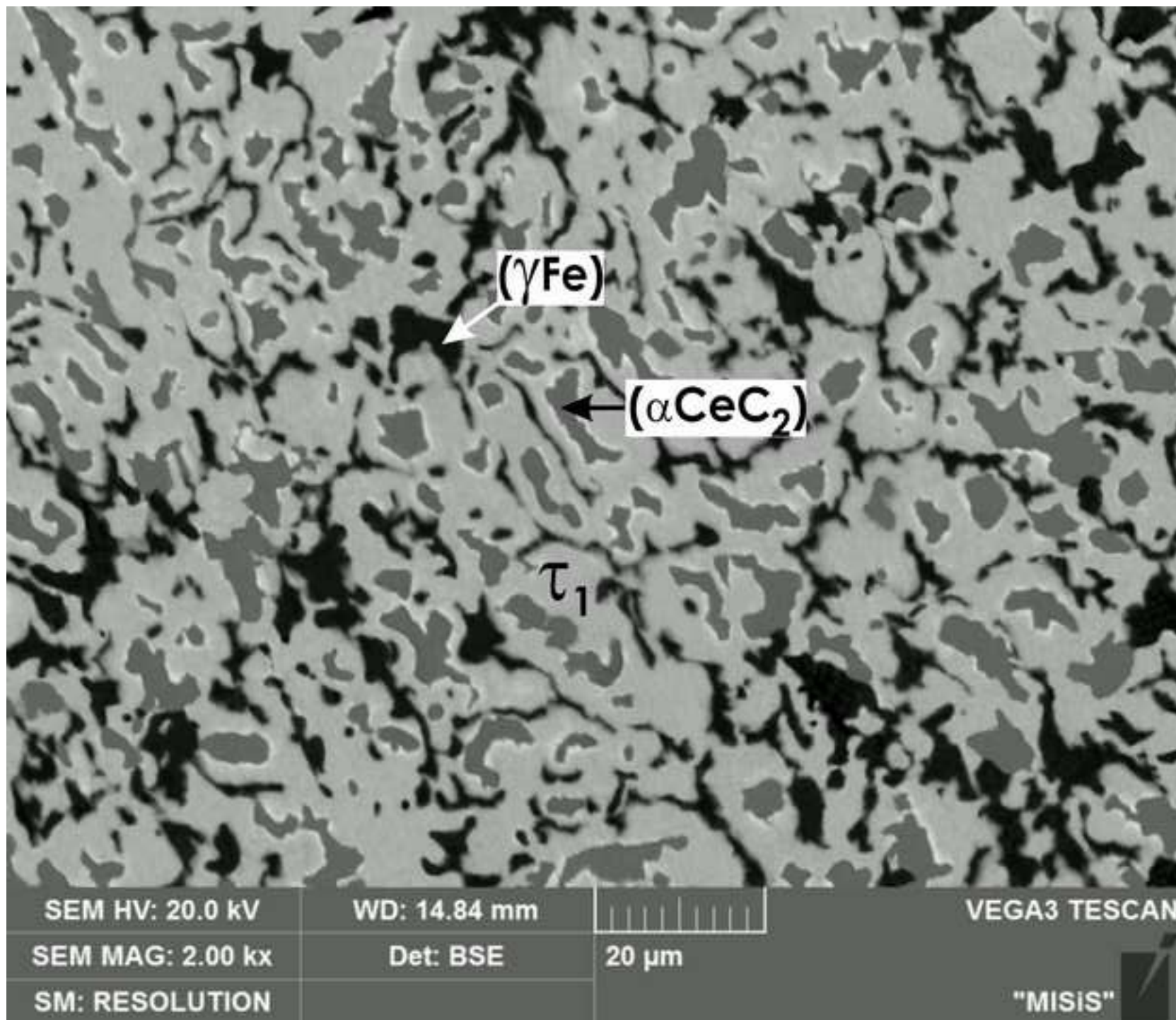
Figure

[Click here to download high resolution image](#)



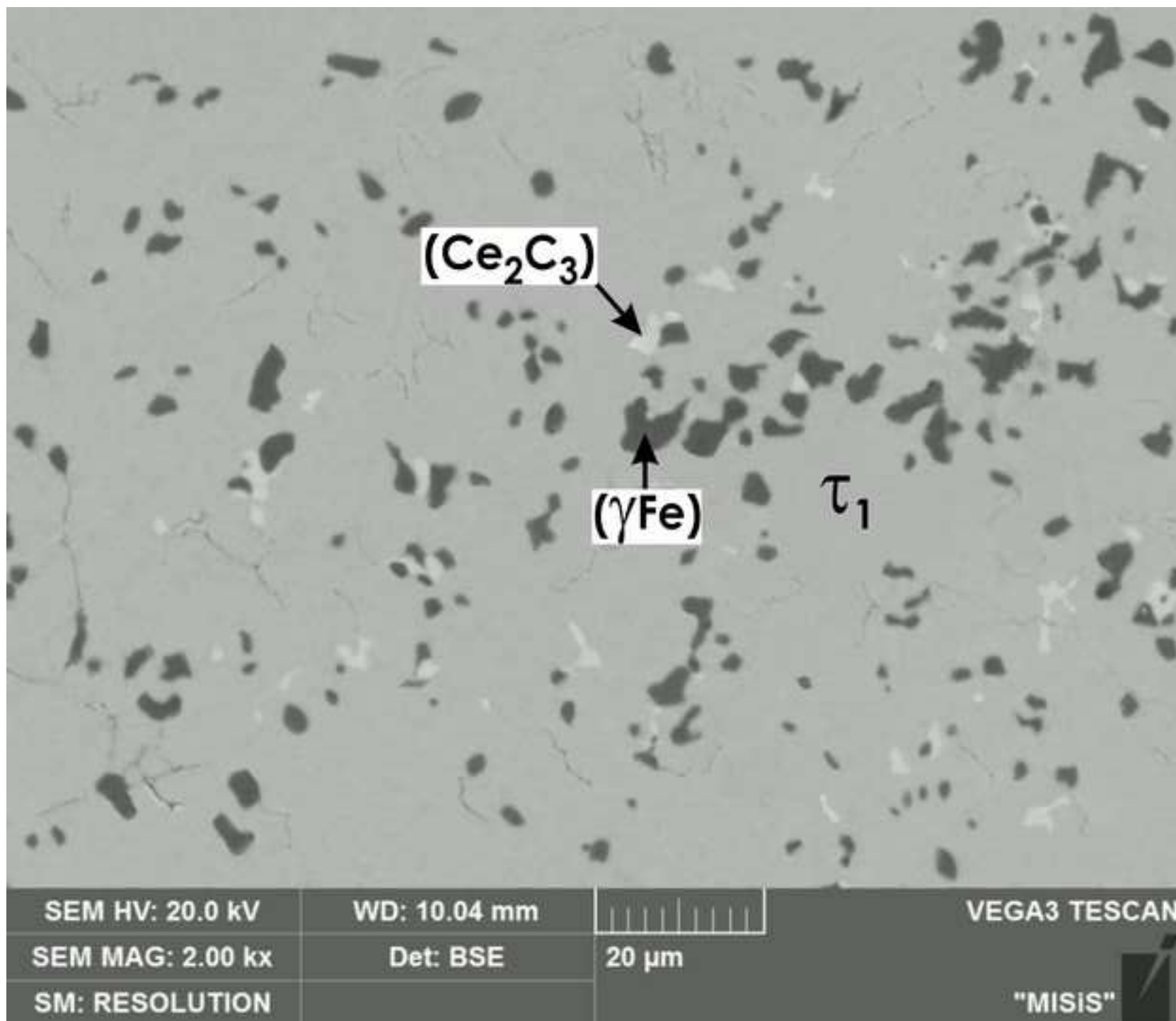
Figure

[Click here to download high resolution image](#)



Figure

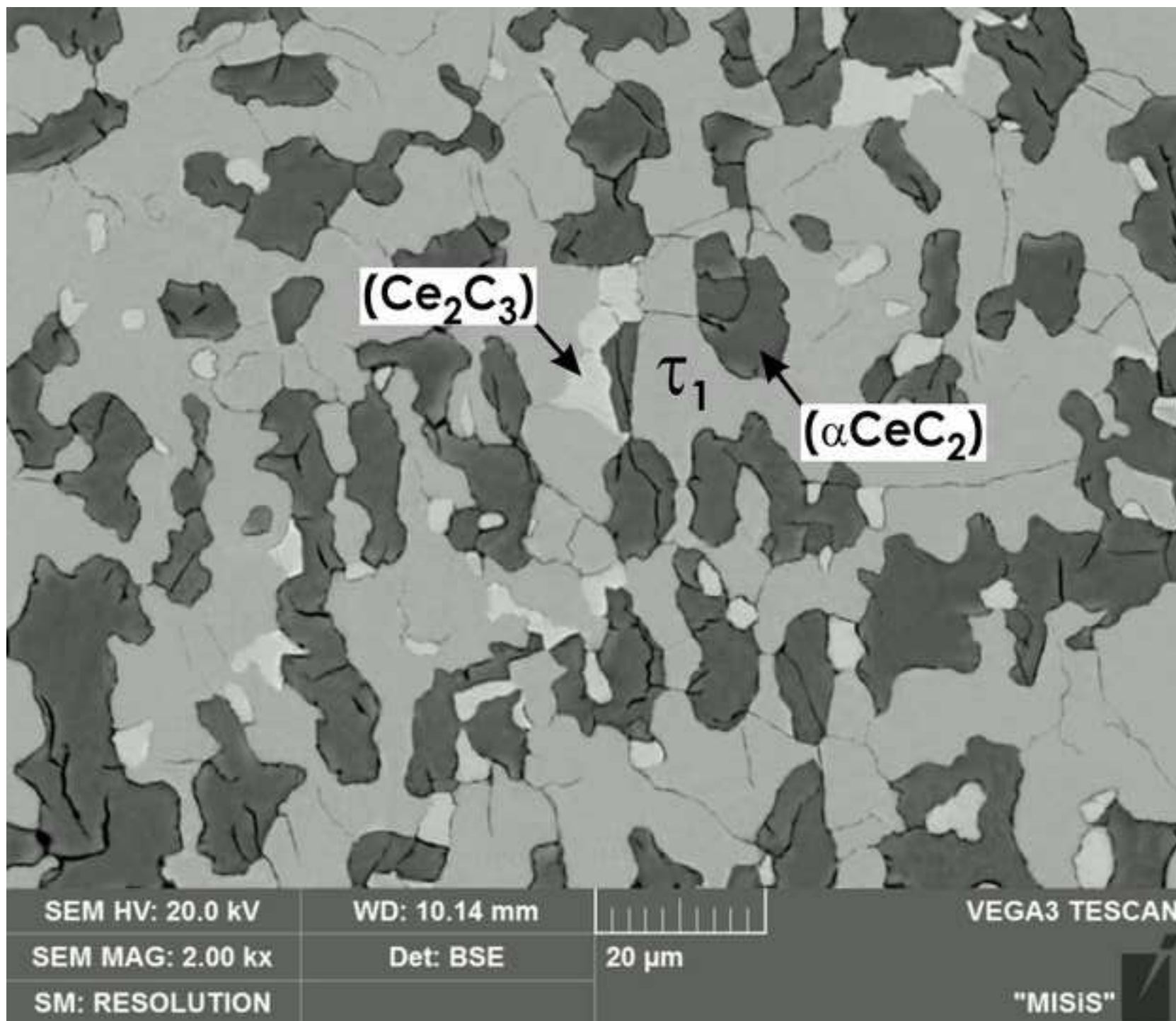
[Click here to download high resolution image](#)





Figure

[Click here to download high resolution image](#)



Figure

[Click here to download high resolution image](#)

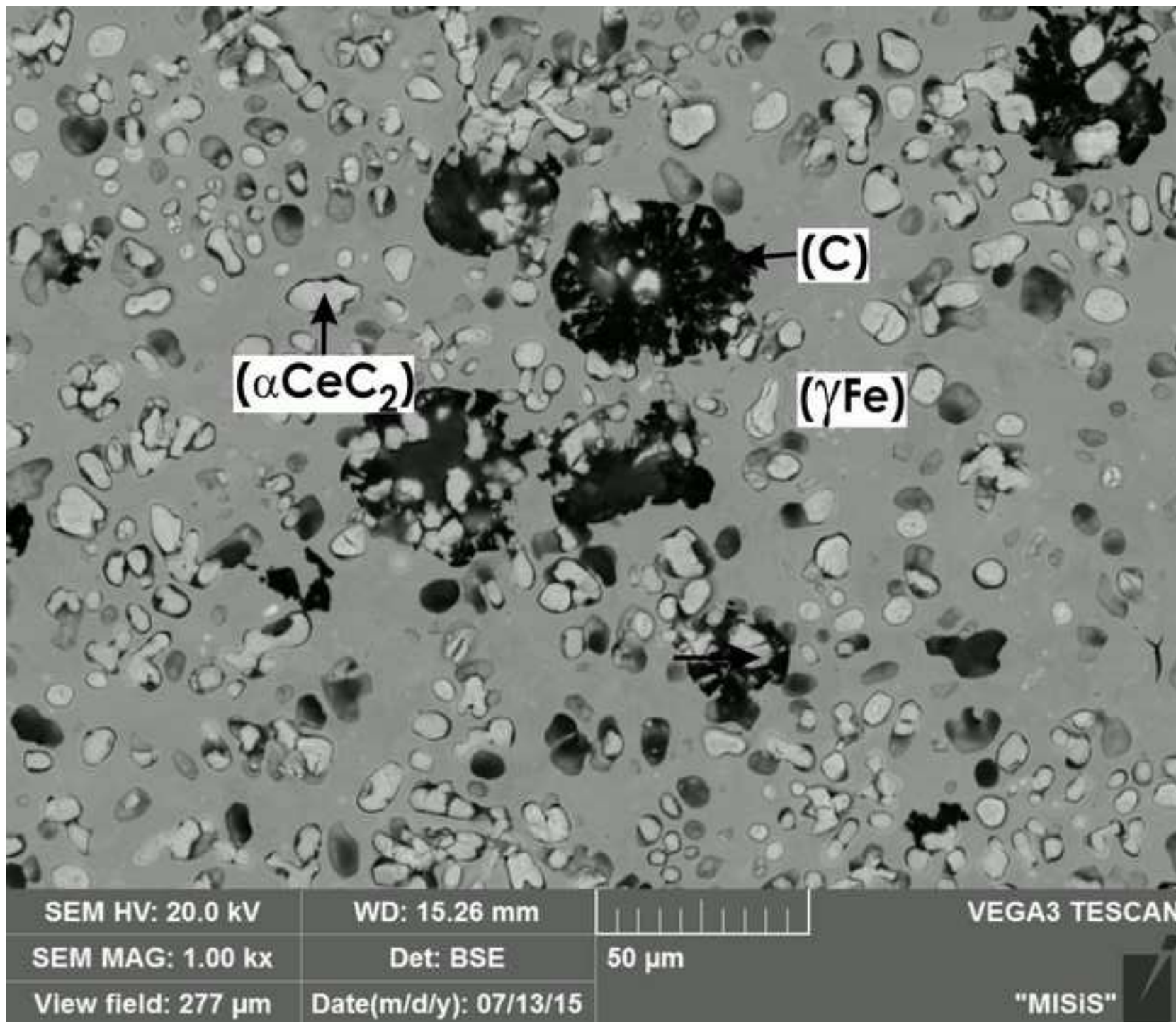


Figure  
[Click here to download high resolution image](#)

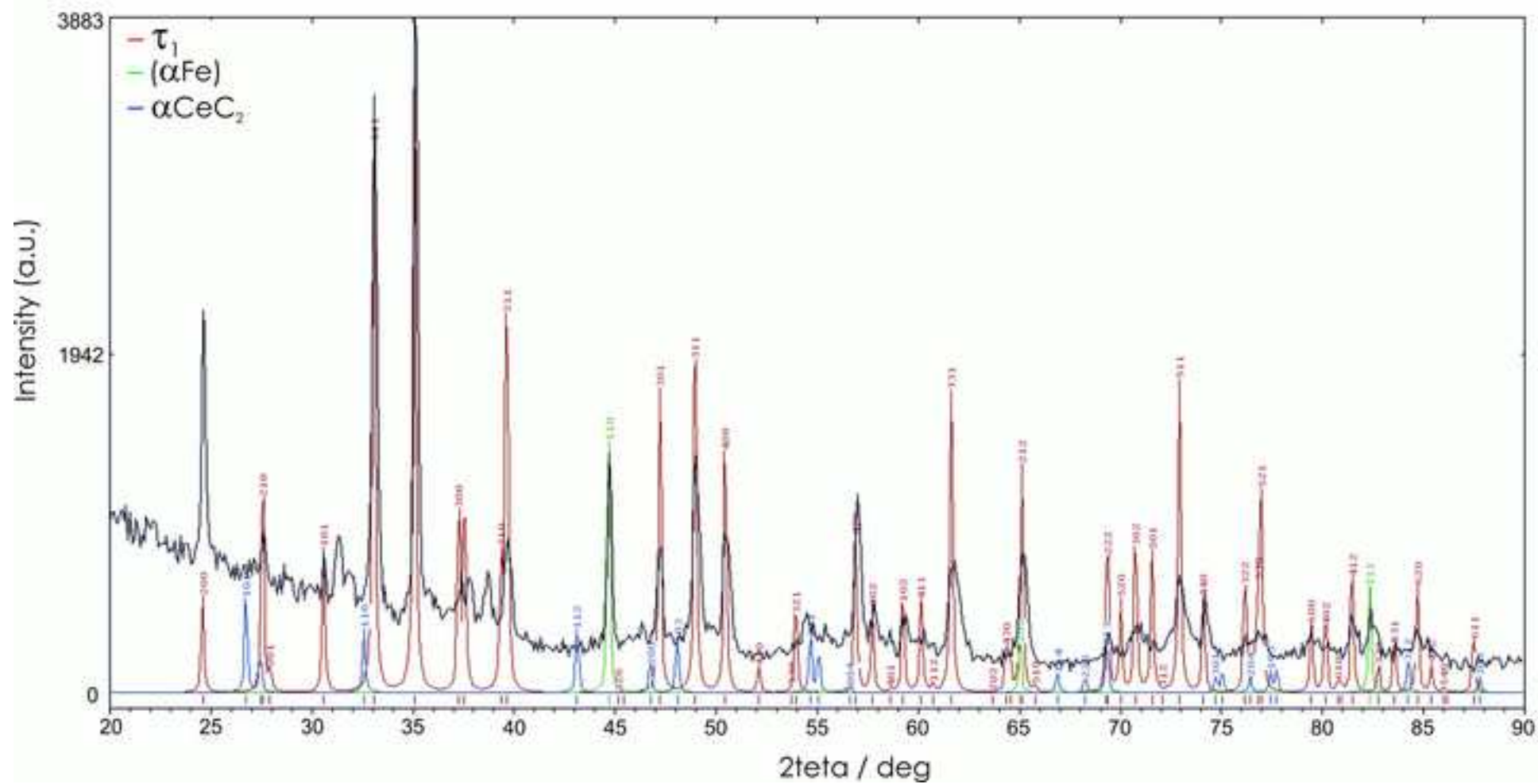


Figure  
[Click here to download high resolution image](#)

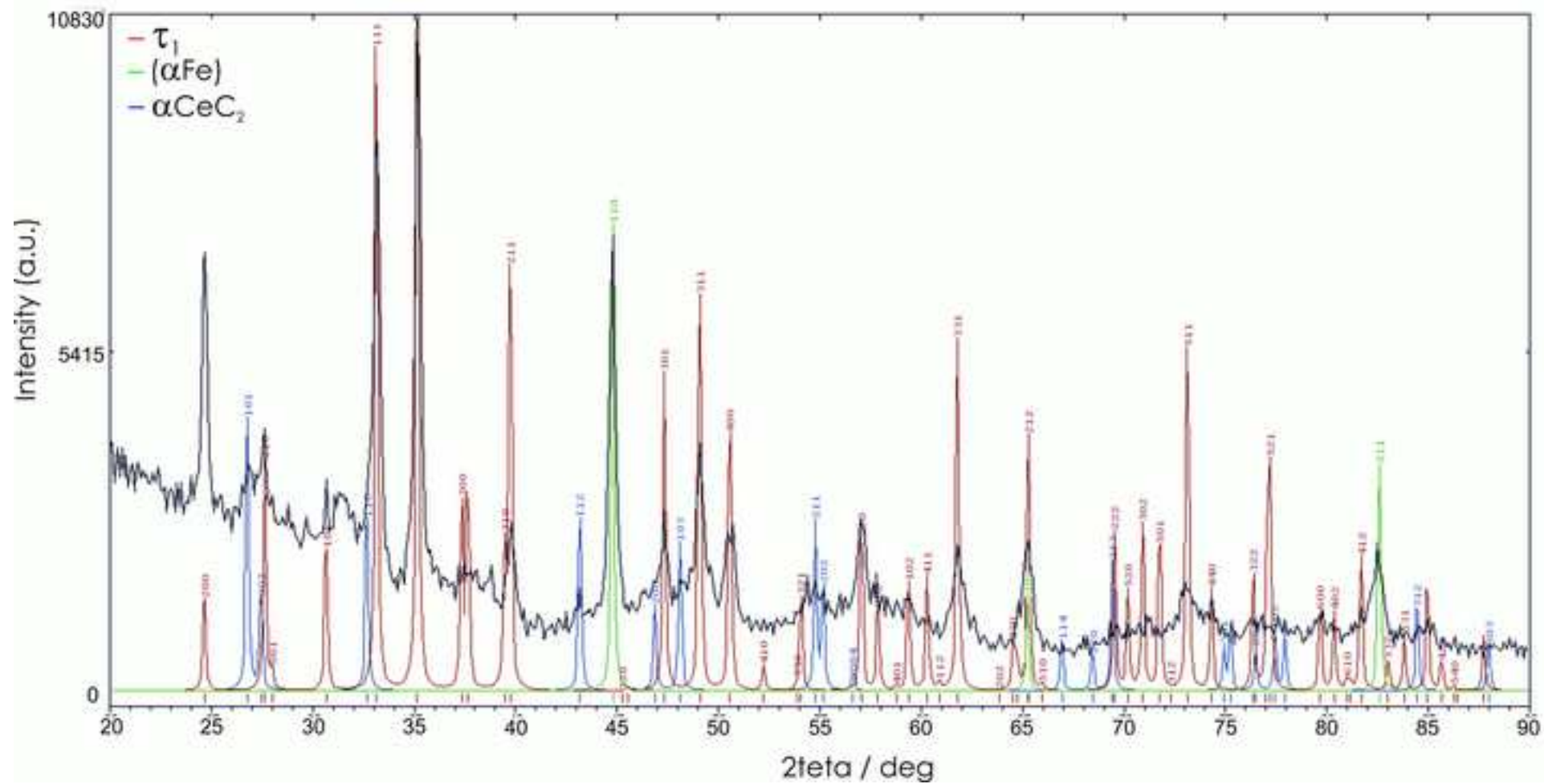


Figure  
[Click here to download high resolution image](#)

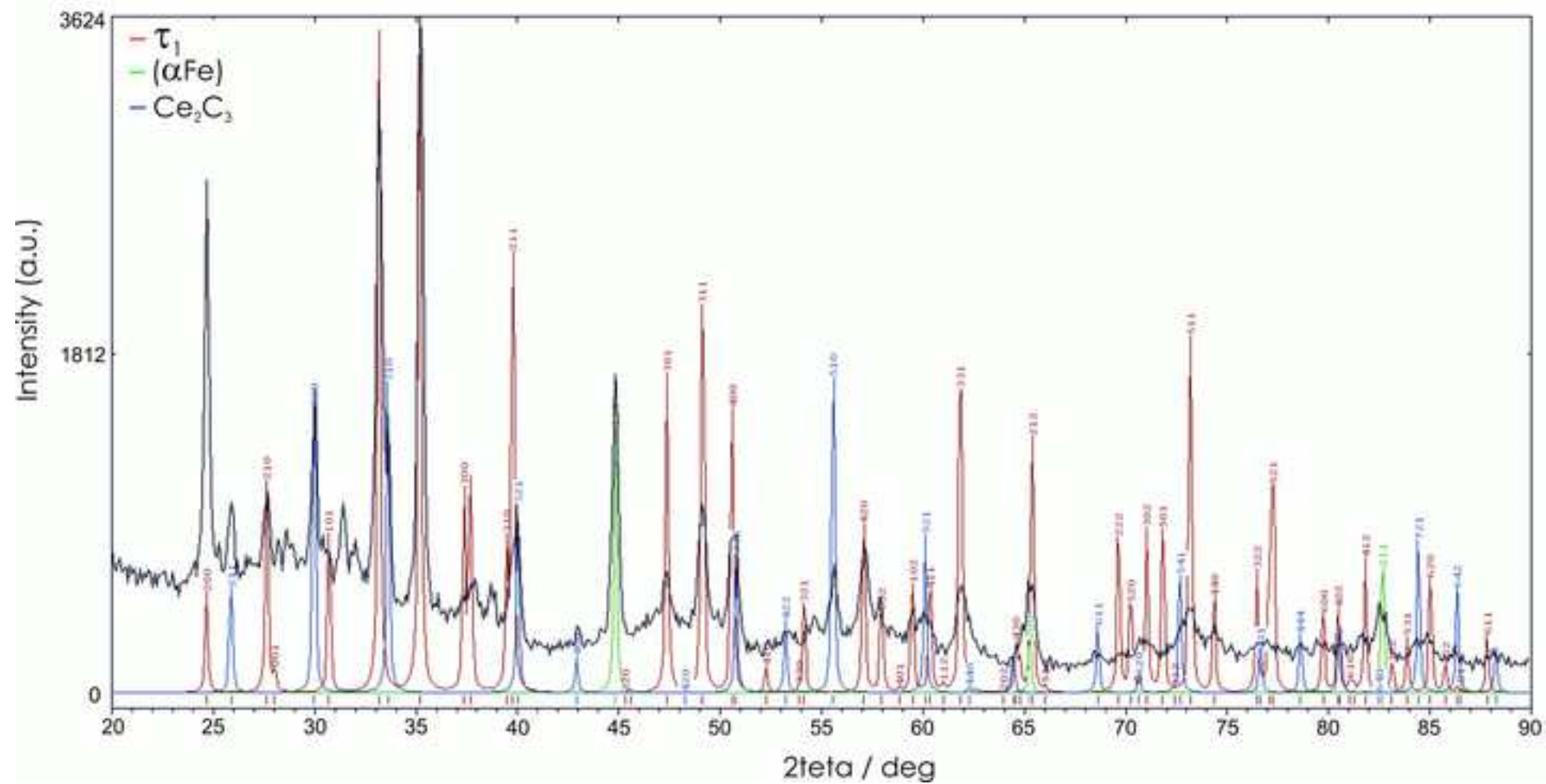


Figure  
[Click here to download high resolution image](#)

